Article

Not peer-reviewed version

New Polymorph of β-Cyclodextrin with a Higher Bioavailability

Askar K. Gatiatulin *, Ilya S. Balakhontsev, Sofia M. Talashmanova, Marat A. Ziganshin, Valery V. Gorbatchuk

Posted Date: 4 December 2023

doi: 10.20944/preprints202312.0111.v1

Keywords: beta-cyclodextrin; polymorphism; bioavailability; polymorphic transition; dissolution rate

Article

New Polymorph of β-Cyclodextrin with a Higher Bioavailability

Askar K. Gatiatulin *, Ilya S. Balakhontsev, Sofia M. Talashmanova, Marat A. Ziganshin and Valery V. Gorbatchuk

A.M. Butlerov Institute of Chemistry, Kazan Federal University, 18 Kremlevskaya, 420008 Kazan, Russia
* Correspondence: agatiatu@kpfu.ru

Abstract: A new polymorph of anhydrous β-cyclodextrin (polymorph III) was obtained and characterized for the first time using powder X-ray diffraction, infrared spectroscopy and thermal analysis. Solution enthalpy and time of dissolution in water were determined by solution calorimetry for this polymorph and compared with those of dried commercial form of β-cyclodextrin (polymorph I), its amorphous form and 2-hydroxypropyl-β-cyclodextrin. Specific heat capacity of polymorphs I and III was determined by differential scanning calorimetry in the wide range of temperatures, which gives enthalpy and Gibbs energy of polymorphic transition at 298 K. Affinity of polymorph III and 2-hydroxypropyl-β-cyclodextrin for water was characterized by determination of their hydration isotherms, which gives the values of hydration Gibbs energy. Being energy-rich, the found new polymorph of β-cyclodextrin has a significantly higher dissolution rate and an in-creased affinity for water compared with the dried commercial form of β-cyclodextrin. Such properties make the new polymorph promising in industrial applications for guest inclusion in aqueous solutions and pastes and may be a desirable alternative for water-soluble β-cyclodextrin derivatives.

Keywords: beta-cyclodextrin; polymorphism; bioavailability; polymorphic transition; dissolution rate

1. Introduction

The solubility of natural cyclodextrins is a key issue when they used to reduce the negative effects of substances dissolved in water. Natural cyclodextrins are widely applied in pharmaceutics, food industry, textiles and cosmetics [1–4] because of their ability to encapsulate various guests into molecular cavity. The most widely used cyclodextrin is β-cyclodextrin (βCD), which accounts for about half of the pharmaceutical applications.[5] The important property of cyclodextrins is their ability to solubilize poorly soluble drugs,[6,7] which requires a cyclodextrin form with a high dissolution rate. This is a problem for βCD that has a relatively poor solubility and slow rate of dissolution in water.[8] The increased dissolution kinetics can be achieved using the metastable polymorphic form of the substance.[9,10] So, a search of high-energy polymorphic forms of βCD may be of practical importance.[11]

Polymorphism of guest-free βCD is significantly less studied than crystalline patterns of its inclusion compounds which show a wide variety of packing types.[12–14] Relatively stable βCD form of low energy and solubility was prepared from its aqueous solution heated by laser beam.[15] Channel-type (columnar) polymorph (named in this work as Polymorph II) of anhydrous βCD was formed by precipitation from the acetone-water solution [16] and by treatment of polymer inclusion complexes with organic solvents.[17] Some data on βCD without guest and water can be found in CCDC database (e.g. No. 762697) but it presents host packing in an inclusion compound where disordered molecules of guest and solvent were removed with software methods. [18] Generally, anhydrous βCD cannot be studied using single-crystal X-ray diffraction (SCXRD) because its crystals tend to crack during the drying. [19, 20]

The phase transition in anhydrous βCD has been observed previously in DSC experiment at 483–513 K [21] but the nature of this transition has not been investigated. In the present work, the product of dry βCD heating to 508 K was first characterized as a new polymorph in the present work by its thermal stability, heat capacity, thermokinetics of corresponding polymorphic transition,

 doi:10.20944/preprints202312.0111.v1

powder XRD pattern, hydration isotherm, the rate and enthalpy of dissolution in water. Besides, the dissolution properties of 2-hydroxypropyl-beta-cyclodextrin (HPβCD), which is widely used for solubilization and guest inclusion in solutions,[6,22,23] and amorphous βCD were studied for comparison to reveal the advantages of the new βCD polymorph.

2. Materials and Methods

2.1. Materials

β-Cyclodextrin (βCD), Sigma Aldrich, Cat. No. C4767, and (2-hydroxypropyl)-β-cyclodextrin (HPβCD, *Mw* ~1540, substitution degree of 1.0), Sigma Aldrich, Cat. No. 389145, were dried before experiments for 8 h in vacuum of 100 Pa at 393 K. For βCD, this gives the initial anhydrous form (polymorph I). In dried CDs, the hydration level was less than 1% wt. according to thermogravimetry data. To prepare the high-temperature polymorph (polymorph III), the initial form (polymorph I) was heated to 508 K in a thermal analyzer (see below) in an argon flow of 75 mL min^{-1} at a rate of 10 K min^{-1} and then cooled immediately to 303 K at the same rate. For PXRD measurement with the indexing of obtained pattern, a larger amount of polymorph III was prepared by heating polymorph I at 505 K for 5 min in ventilated oven and then cooling in air to room temperature in the presence of desiccant ().

The amorphous βCD was prepared by ball milling of the initial dried βCD using vibration ball mill Narva DDR GM 9458 (30 W, 50 Hz) and drying for 8 h in vacuum of 100 Pa at 393 K.

To determine hydration isotherms by CDs and X-ray powder diffractograms of βCD hydrates, the samples of anhydrous CDs were equilibrated for 120 h at 298 K with the vapors of saturated aqueous solutions of different inorganic compounds having a known water activity (humidity) or with saturated water vapor, as described previously.[24] Change of mass due to hydration of CD samples was determined gravimetrically. For recrystallization in water vapor, anhydrous βCD sample was equilibrated with the saturated vapor of distilled water for 24 h. To recrystallize from aqueous solution, 30 mg of dry βCD polymorph was dissolved in 2 mL of distilled water at room temperature. The solutions in both cases were kept in air at room temperature till the powders of βCD hydrate were formed.

2.2. Thermal Analysis and Thermal Kinetics

For thermal analysis, a combined method of thermogravimetry and differential scanning calorimetry (TG/DSC) was applied using thermal analyzer Netzsch STA 449 C Jupiter. Samples were heated at a rate of 10 K min^{-1} in an argon flow of 75 mL min^{-1}. In full cycle TG/DSC experiment the sample was also cooled at 10 K min^{-1} in the same argon flow. To obtain the kinetic parameters, heating rates of 4, 10, and 30 K min^{-1} were used under the same conditions. From the data obtained in this experiment, the kinetic parameters of polymorphic transition were calculated using the Netzsch Thermokinetics 3.1 software.

The heat capacity of βCD polymorphs was measured using Netzsch DSC204 F1 Phoenix calorimeter with a sapphire disk as a standard, as described elsewhere.[25]

2.3. Powder X-Ray Diffraction (PXRD)

Powder diffractograms were obtained using Rigaku MiniFlex 600 diffractometer with a D/teX Ultra detector. In this experiment, Cu Kα radiation (30 kV, 10 mA) was used, Kβ radiation was attenuated with Ni filter. The experiments were made without sample rotation at room temperature in the reflection mode, at rate of 10 ° min^{-1} for anhydrous CD samples and at 5 ° min^{-1} for hydrates. The diffractograms were determined also with an additive of standard silicon powder SRM 640d, and corresponding corrections were applied to the patterns obtained. The samples of anhydrous βCD were studied in a standard glass holder immediately after being taken out to air with humidity of 20-40%.

For indexing of polymorph III pattern, the PXRD experiment was held also at the increased X-ray tube power (30 kV, 20 mA) with scanning rate of 0.5 ° min^{-1} and sample rotation (80 rpm). To

 doi:10.20944/preprints202312.0111.v1

avoid hydration of βCD sample in a course of this experiment, the desiccant (freshly dried molecular sieves) was placed in the diffractometer camera. The indexing of pattern was performed using EXPO2014 software with further Rietveld refinement. [26,27]

2.4. Solution Calorimetry

The dissolution enthalpies and kinetics were measured at 298.15±0.01 K using the semiadiabatic calorimeter described earlier.[28] In this experiment, sample of 30 mg was dissolved in 100 mL of distilled water. For each CD form, the dissolution experiment was carried out three times, and average parameters of calorimetric curves were calculated.

2.5. Infrared Spectroscopy

Infrared (IR) spectra were collected using Bruker Vertex 70 Fourier-transform infrared spectrometer, which was purged by dry air before the experiment to remove the atmospheric humidity. The interferograms were recorded with 64 scans and a resolution of 2 cm^{-1}. Spectra of solid samples were recorded using attenuated total reflection MIRacle accessory with germanium crystal (PIKE Tech.).

3. Results

3.1. Preparation of Polymorph III

The high-temperature polymorph (polymorph III) was prepared by heating the initial anhydrous βCD (polymorph I) to 508 K in argon flow in TG/DSC experiment. Corresponding TG/DSC curves are given in Figure 1. During the first heating of polymorph I, an endothermic effect is observed with onset point at 495 K (Figure 1). The enthalpy of such effect is ΔH_{tr} = 16.5 kJ mol^{-1}. This effect is absent in the second heating run for the product of polymorph I heating to 508 K and cooling (Figure 1) and no peaks of phase transition can be seen in the corresponding DSC cooling curve in a separate TG/DSC experiment (Figures A7, A8), what indicates irreversibility of the observed transition.

According to TG data, βCD has no mass loss in the range of 473–513 K (Figure 1). Thus, the endothermic process at these temperatures corresponds to a polymorphic transition leading to the formation of the new polymorph III. For this high-temperature polymorph III, the onset point of thermal destruction is 526 K, which is by 8 K lower than that of the initial form. The lower thermal stability of polymorph III can be explained by its higher energy than that of the initial βCD form.

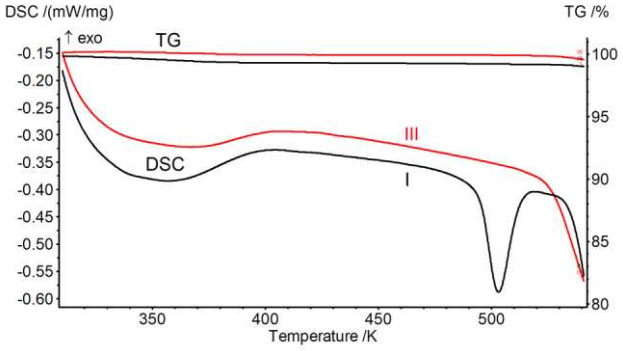

Figure 1. Curves of TG/DSC analysis of polymorphs I and III with the heating rate of 10 K min^{-1}.

To differentiate the endothermic polymorphic transition at 495 K from the thermal degradation of βCD, the dependence of the observed transition on heating rate was determined in DSC experiment and corresponding activation energy E_a was calculated using model-free and optimal model methods.[29,30] The experimental data and description of calculation details are given in Appendix A. For this transition, model-free Ozawa-Flynn-Wall and Friedman methods give the

Preprints (www.preprints.org) | NOT PEER-REVIEWED | Posted: 4 December 2023 doi:10.20944/preprints202312.0111.v1

activation energy E_a of 430 and 350 kJ mol^{-1}, respectively, in the conversion range of 0.1–0.7. The optimal thermokinetic model is the Prout-Tompkins equation with E_a = 430 kJ mol^{-1} and process order of n = 1.92. These E_a values are in 3-4 times higher than the activation energy E_a =105 kJ mol^{-1} of the βCD thermal degradation reaction,[31] which confirms a different nature of the observed endothermic effect.

The structural changes upon polymorphic transition were studied using the powder X-ray diffraction method. For this, diffraction patterns were determined for polymorph I, polymorph III and products of its saturation with water vapor having relative humidity of 33% (water activity a_w = 0.33), its recrystallization in water vapors at a_w = 1.0 (both at 298 K) and from aqueous solution (Figure 2). Polymorph III for this experiment was prepared by two methods: by heating polymorph I to 508 K and cooling in argon flow and, in a larger scale, by heating to 505 K and cooling in air. Both methods give the samples with nearly the same PXRD pattern (Figure 2b,c, A9).

The diffractograms obtained indicate an essentially different packing of high-temperature polymorph III (Figure 2b,c) than that of the initial polymorph I (Figure 2a). Both these patterns do not coincide with diffractogram of channel-type polymorph II [16] by their characteristic peaks, Table 1. The indexing of high-temperature polymorph III diffractogram (Figure A5) for the sample prepared by heating polymorph I to 505 K and cooling in air gives a triclinic cell with parameters of a = 17.09 Å, b = 15.12 Å, c = 11.76 Å, α = 109.5°, β = 95.8°, γ = 70.6°, Table 1, with R_{wp} = 5.466. The cell volume of this high-temperature polymorph is V = 2704 Å^3, which is more compact than the initial dried βCD form having V = 2894 Å^3 [24]. For comparison, polymorph II has a hexagonal cell [17] with volume V = 3069 Å^3, Table 1.

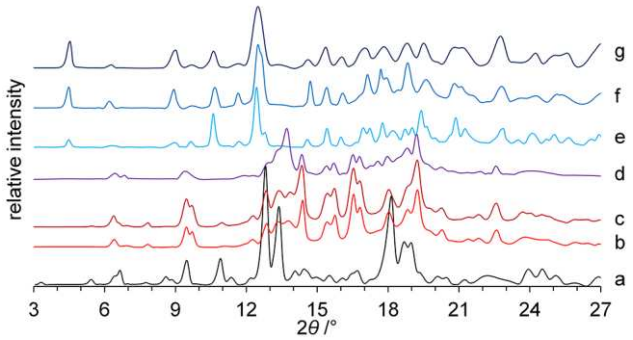

Figure 2. PXRD patterns at room temperatures of (a) polymorph I; (b) polymorph III prepared by heating polymorph I to 508 K and cooling in argon flow; (c) polymorph III prepared by heating polymorph I to 505 K and cooling in air; the products of polymorph III (d) hydration at water activity a_w = 0.33, (e) recrystallization in water vapors at a_w = 1.0 and (f) recrystallization from aqueous solution at 298 K; (g) diffractogram of the saturated hydrate βCD·11.2H_2O.

Table 1. Structural parameters and properties of anhydrous βCD polymorphs.

Polymorph	**I**	**II**	**III**
Preparation method	Drying of βCD hydrate (Form I)	Precipitation from the acetone-water solution [16]; treatment of polymer inclusion complexes with organic solvents [17]	Heating of polymorph I to 505-508 K
Characteristic PXRD peaks (2θ), °	5.5, 6.5, 9.6, 11.0, 12.9, 13.5, 14.1, 16.9, 18.2, 22.3 [32]	6.7, 11.8, 17.8 [16]	9.5, 13.4, 14.4, 15.7, 16.8, 19.2, 22.6
Crystal system	monoclinic	hexagonal	triclinic
Cell parameters	a = 13.703 Å	a = 15.34 Å	a = 17.09 Å

Preprints (www.preprints.org) | NOT PEER-REVIEWED | Posted: 4 December 2023 doi:10.20944/preprints202312.0111.v1

	b = 16.065 Å c = 13.163 Å β = 92.69 ° [24]	c = 15.06 Å [17]	b = 15.12 Å c = 11.76 Å, α = 109.5 ° β = 95.8 ° γ = 70.6 °
Cell volume, Å³	2894	3069	2704
Onset point of thermal degradation, K	534	478-483 [17]	526

Hydration of polymorph III at water activity a_w = 0.33 and 298 K gives minor changes in its diffraction pattern (Figure 2d) without change of its main packing type. In saturated water vapors at a_w = 1.0, this polymorph forms a mixture of aqueous βCD solution and its solid hydrate, unlike the initial polymorph I, which remains in a solid state state under these conditions.[32,33] The products of such recrystallization in water vapors (Figure 2e) and recrystallization of the same high-temperature polymorph III from aqueous solution (Figure 2f) without drying have practically the same packing as the saturated hydrate βCD·11.2H_2O prepared by saturation of the polymorph I at a_w = 1.0 (Figure 2g). So, no chemical reactions occur in anhydrous βCD upon heating to 508 K, which is 5 K above the peak point of polymorphic I→III transition. The absence of chemical changes is also confirmed by the identity of the IR spectra of both polymorphs (Appendix A).

3.2. Dissolution rate

Being the high-temperature form produced by endothermic transition, polymorph III is expected to have a higher dissolution rate. To study the dissolution rate in water for this polymorph and the other studied anhydrous forms of βCD and dried HPβCD for comparison, the method of solution calorimetry was chosen, which can estimate the time of fast dissolution processes.[34]

Calorimetric curves were determined, Figure 3, for dissolution of polymorphs I and III, and amorphous forms of dried ball-milled βCD and dried HPβCD. The corresponding values of dissolution times t_{soln} and enthalpies ΔH_{soln} are given in Table 2.

Table 2. Dissolution properties of anhydrous forms of βCD and HPβCD at 298 K.

	Dissolution time t_{soln} /s	**Solution enthalpy ΔH_{soln} /kJ mol^{-1}**
Polymorph I	190±15	–86±1
Polymorph III	43±4	–94±1
amorphous βCD [a]	43±4 (90±10)[b]	–111±1
HPβCD *a*	100±10	–144±1

[a] PXRD patterns are given in Appendix A; [b] the total dissolution time with prolonged endothermic effect having negligibly small enthalpy value.

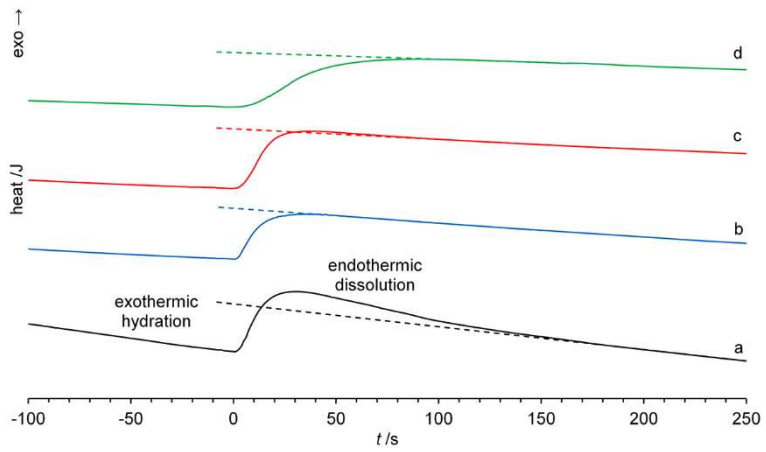

 doi:10.20944/preprints202312.0111.v1

Figure 3. Calorimetric dissolution curves at 298 K of (a) polymorph I, (b) polymorph III, (c) anhydrous amorphous βCD and (d) anhydrous HPβCD. The start of dissolution is at t = 0 s. The dotted lines are the extrapolation of baselines after the end of dissolution effects.

The dissolution of polymorph I includes two processes: exothermic hydration curve of anhydrous βCD and endothermic dissolution of βCD hydrate. These processes have been separately characterized elsewhere [35] and can be seen in a complex shape of polymorph I dissolution curve (Figure 3a). This calorimetric curve demonstrates rather fast exothermic effect in the first 35 s after the start of dissolution with the next prolonged endothermic event for 155 s. The ratio of these thermal effects 3.5:1 corresponds to the values of the determined polymorph I solution enthalpy ΔH_{soln} = –86±1 kJ mol^{-1} and literature data [35] of ΔH_{soln} = –91 kJ mol^{-1} for the same anhydrous βCD form and ΔH_{soln} = +35 kJ mol^{-1} for saturated hydrate βCD·12H$_2$O, which gives the ratio 3.6:1 of βCD hydration and βCD·12H$_2$O hydrate dissolution enthalpies. The composition of saturated βCD hydrate is from the single crystal XRD.[36] This means that hydration and hydrate dissolution events occur not simultaneously in any significant extent but one after another.

The dissolution curve of polymorph III (Figure 3b) performs only the exothermic effect with ΔH_{soln} = –94±1 kJ mol^{-1} within the first 43 s, Table 2. So, its hydration and dissolution are simultaneous. The difference in ΔH_{soln} values of polymorphs I and III at 298 K is 8±2 kJ mol^{-1} is lower than the enthalpy of polymorphic transition +16.5 kJ mol^{-1} with onset at 495 K, Figure 1, which may be caused by the difference in experimental temperatures. The amorphous βCD with dissolution enthalpy of ΔH_{soln} = –111±1 kJ mol^{-1} shows the same dissolution time of 43 s as polymorph III in practically one exothermic step followed by very small but prolonged (t_{soln} = 90±10 s) endothermic effect, which is only ~3% of the total dissolution enthalpy. This may be caused by formation of crystalline βCD hydrate from the minor part of the initial amorphous sample having a higher energy by 17 kJ mol^{-1} than polymorph III.

The dissolution curve of anhydrous HPβCD with ΔH_{soln} = –144±1 kJ mol^{-1} has the same shape as observed for polymorph III but with much higher dissolution time of t_{soln} = 100 s (Figure 3d, Table 2). Thus, the dissolution rate of polymorph III in water is close to that of amorphous βCD, being 4.4 and 2.3 times higher than that of the initial polymorph I and HPβCD, respectively, despite the latter one is amorphous, and its dissolution is more exothermic. A similar difference in the dissolution rates of these forms was also observed visually.

3.3. Thermodynamic properties

The different properties of βCD polymorphs I and III were also observed in DSC experiment where dependences of their molar heat capacity $C_{p,m}$ on temperature T in the range of 343–463 K were determined. This range was chosen because it excludes the influence of water traces in dried argon used to purge CD samples. The obtained plots of $C_{p,m}$ vs. T are given in Figure 4, and the values of $C_{p,m}$ at each studied temperature are given in Appendix A. The molar heat capacity of the initial polymorph I can be described by the equation $C_{p,m} = -1219 + 10.36T - 0.00623T^2$. This equation extrapolated to the temperature T = 298 K gives $C_{p,m}$ = 1316±13 J mol^{-1} K^{-1}, which is slightly lower than 1342±10 J mol^{-1} K^{-1} measured earlier at the same temperature.[37] The molar heat capacity of polymorph III can be described as $C_{p,m} = -884 + 9.05T - 0.00478T^2$. Hence, molar heat capacity of polymorph III is higher, than that of polymorph I in the studied range of temperatures (Figure 4).

Preprints (www.preprints.org) | NOT PEER-REVIEWED | Posted: 4 December 2023 doi:10.20944/preprints202312.0111.v1

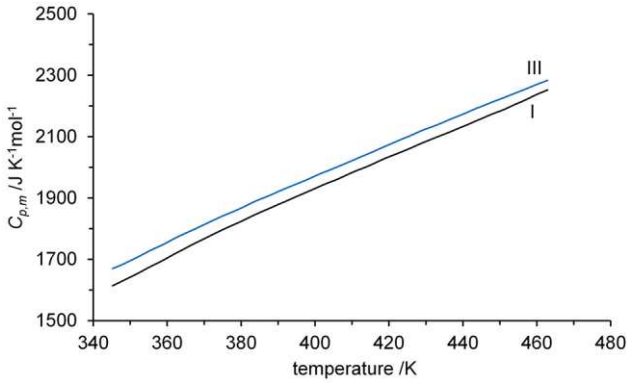

Figure 4. Dependence of molar heat capacity on temperature for βCD polymorphs I and III.

The enthalpy of I→III transition ΔH_{tr} at 298 K can be estimated using Kirchhoff's law by the value of ΔH_{tr}(495K) = 16.5 kJ mol^{-1} determined in DSC experiment (Figure 1) and the difference of heat capacities $\Delta C_{p,m}$ of polymorphs I and III:

$$\Delta H_{tr}(298\ \mathrm{K}) = \Delta H_{tr}(495\ \mathrm{K}) + \int_{495}^{298} \Delta Cp,m(T)dT = 7.1\ (\frac{\mathrm{kJ}}{\mathrm{mol}}) \qquad (1)$$

The calculated value of ΔH_{tr}(298 K) coincides with the difference in enthalpies of polymorphs I and III dissolution in water at 298 K, which is equal to 8±2 kJ mol^{-1}, Table 2.

Since the endothermic process in anhydrous βCD at 495 K is the transition from polymorph I to polymorph III followed by melting of βCD at 774 K,[31] this polymorphic transition is enantiotropic with zero value of transition Gibbs energy ΔG_{tr}(495 K) = 0 according to the heat-of-transition rule of Burger and Ramberger.[38] Hence, the value of polymorphic transition entropy at its onset point is equal to ΔS_{tr}(495 K) = 33 J mol^{-1} K^{-1}. So, the entropy of I→III transition at 298 K can be calculated:

$$\Delta S_{tr}(298\ \mathrm{K}) = \Delta S_{tr}(495\ \mathrm{K}) + \int_{495}^{298} \frac{\Delta Cp,m(T)}{T} dT = 8.2\ (\frac{J}{mol \cdot K}) \qquad (2)$$

This gives the positive value of transition Gibbs energy at standard temperature, ΔG_{tr}(298 K) = 4.7 kJ mol^{-1}, which means that polymorph III has a higher Gibbs energy than polymorph I at 298 K. Such relationship can explain the higher dissolution rate of polymorph III and, respectively, its higher bioavailability.

3.4. Affinity for water

To compare the affinity of polymorph III for water with that of polymorph I and HPβCD, the hydration isotherms were measured for polymorph III and HPβCD using their equilibration with water vapors of fixed humidity at 298 K and gravimetric determination of hydrate composition. Hydration isotherm of polymorph I has been determined elsewhere.[33] The isotherms were fitted using Hill equation, as described earlier.[39] The used equation and approximation parameters are given in Appendix A. These are inclusion capacity *S*, water activity at 50% saturation extent $a_{0.5S}$, which is a hydration threshold, and cooperativity parameter for separate inclusion steps.

Hydration of polymorph III occurs in two steps (Figure 5b), corresponding to the inclusion capacity *S* of 2.5 and 1.6 mol water per mol βCD with hydration threshold $a_{0.5S}$ at 0.09 and 0.30, respectively. Such steps means that hydration of polymorph III produces a phase transition, which may be induced by inclusion inside βCD cavity because of the uptake of 4 water molecules at a_w = 0.33 does not produce does not show significant changes in polymorph III PXRD pattern (Figure 2d). For comparison, 4.5 and 7 water molecules have such inclusion type in βCD·9.4H_2O and βCD·12.3H_2O single crystals, respectively.[35] Hydration of polymorph III at a_w = 0.43 gives a mixture of aqueous solution and crystalline βCD hydrate with a total βCD/water molar ratio of 1:20.5, where the liquid phase is observed visually. Such behavior was not observed under the same conditions for polymorph I, which cannot sorb more water than needed to form its hydrates in two steps (Figure

Preprints (www.preprints.org) | NOT PEER-REVIEWED | Posted: 4 December 2023 doi:10.20944/preprints202312.0111.v1

5b), corresponding to the inclusion capacity S of 9.2 and 2.2 mol per mol βCD with hydration threshold $a_{0.5S}$ at 0.26 and 0.97, respectively.[33]

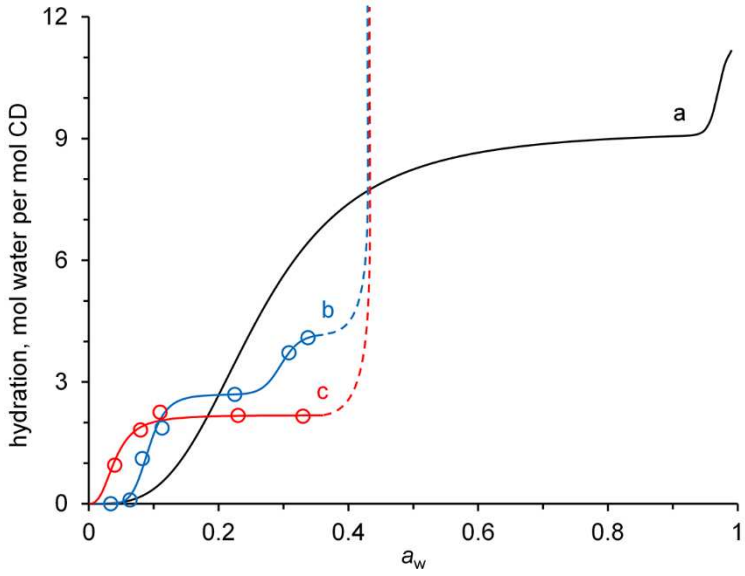

Figure 5. Water sorption isotherms on (a) polymorph I [33] and (b) polymorph III, and on (c) anhydrous HPβCD at 298 K. T = 298 K. The dotted line corresponds to the formation of liquid solution.

The isotherm of HPβCD hydration (Figure 5c) performs only one step with a lower hydration capacity S = 2.2 mol mol^{-1} and hydration threshold of $a_{0.5S}$=0.04. This isotherm also becomes vertical at a_w = 0.43 with HPβCD giving a drop of its liquid aqueous solution. So, this βCD derivative is more water soluble than the earlier studied HPβCD with a lower substitution ratio of 0.6, which does not dissolve in water vapors even at a_w = 1.[40]

The affinity of the studied CDs for water can be characterized by their hydration Gibbs energy ΔG_h, which was calculated for each step using equation:

$$\Delta G_h = RT \ln a_{0.5S}$$

This equation gives Gibbs energy [39] of water transfer from its pure liquid to stable hydrate with the inclusion capacity S. The values of ΔG_h for the first and second hydration step of polymorph III are –5.9 and –3.0 kJ per 1 mol of water, respectively. HPβCD has this value of ΔG_h = –7.9 kJ mol^{-1}. For comparison, two steps of polymorph I hydration correspond to ΔG_h values of –3.3 and –0.1 kJ mol^{-1}, respectively.[33] So, the affinity for water changes in order: HPβCD > polymorph III > polymorph I. While as HPβCD is well soluble in water (>600 mg mL^{-1}),[41] a similar good solubility could be expected for polymorph III. Still, the equilibrium solubility of polymorph III is restricted by ability of βCD to recrystallize into its saturated hydrate having poor solubility of 18.4 mg mL^{-1},[41] which was observed visually for III in water vapors at activity of a_w = 0.43 as mentioned above. Such dissolution-crystallization behavior can be useful for a preparation of inclusion compounds in pastes using small amount of water or for a quick removal of undesirable compounds from aqueous solution by their complexation with βCD using much faster dissolution of its polymorph III. This property makes polymorph III a promising alternative to the more expensive synthetic derivatives of cyclodextrins.

4. Conclusions

The new polymorph III of β-cyclodextrin was prepared through endothermic transition by heating of the dried commercial form of β-cyclodextrin (polymorph I). The absence of chemical changes in β-cyclodextrin by this treatment was proved by its IR spectra and PXRD patterns after its hydration. Polymorph III has a triclinic cell with an essentially different packing than that of

polymorph I. Polymorph III is energy-rich: the I→III polymorphic transition has a positive enthalpy of +8 kJ mol^{-1} and Gibbs energy of +4.7 kJ mol^{-1} at 298 K. The dissolution of polymorph III in liquid water is 4.3 and 2.3 times faster than dissolution of polymorph I and hydroxypropyl-β-cyclodextrin (HPβCD), respectively, under the same conditions. Polymorph III dissolves in water vapors at the same humidity as the highly water-soluble HPβCD and has a higher affinity for water with a more negative hydration Gibbs energy than polymorph I. Thus, the new polymorph can be used for preparation of inclusion compounds in pastes or for a quick removal of undesirable compounds from water being a cheaper alternative to the chemically modified β-cyclodextrin.

Supplementary Materials: The following supporting information (thermokinetic analysis of the polymorphic transition; PXRD data for Polymorph III and amorphous βCD/HPβCD; IR spectra for βCD polymorphs I and III; Molar heat capacity data for βCD polymorphs I and III; Parameters of hydration isotherms) can be downloaded at the website of this paper posted on Preprints.org.

Author Contributions: AKG conceptualization, formal analysis, writing—original draft; ISB investigation; SMT investigation; MAZ writing—review and editing; VVG supervision, writing—review and editing.

Funding: The work was supported by the RSF grant no. 22-23-00367.

Institutional Review Board Statement: Not applicable.

Informed Consent Statement: Not applicable.

Conflicts of Interest: The authors declare no conflict of interest.

Data Availability Statement: The data that support the findings of this study are available from the corresponding author upon reasonable request.

References

1. Fenyvesi, E.; Szente, L. Cyclodextrin in Starchy Foods. *Acta Aliment.* **2021**, *50*, 417–432, doi:10.1556/066.2021.00051.
2. Morin-Crini, N.; Fourmentin, S.; Fenyvesi, É.; Lichtfouse, E.; Torri, G.; Fourmentin, M.; Crini, G. 130 Years of Cyclodextrin Discovery for Health, Food, Agriculture, and the Industry: A Review. *Environ. Chem. Lett.* **2021**, *19*, 2581–2617, doi:10.1007/s10311-020-01156-w.
3. Gonzalez-Gaitano, G.; Isasi, J.R.; Velaz, I.; Zornoza, A. Drug Carrier Systems Based on Cyclodextrin Supramolecular Assemblies and Polymers: Present and Perspectives. Curr. Pharm. Des. 2017, 23, 411–432, doi:10.2174/1381612823666161118145309.
4. Ferreira, L.; Mascarenhas-Melo, F.; Rabaça, S.; Mathur, A.; Sharma, A.; Giram, P.S.; Pawar, K.D.; Rahdar, A.; Raza, F.; Veiga, F.; et al. Cyclodextrin-Based Dermatological Formulations: Dermopharmaceutical and Cosmetic Applications. *Colloids Surfaces B Biointerfaces* **2023**, *221*, 113012, doi:10.1016/j.colsurfb.2022.113012.
5. Puskás, I.; Szente, L.; Szőcs, L.; Fenyvesi, É. Recent List of Cyclodextrin-Containing Drug Products. *Period. Polytech. Chem. Eng.* **2023**, *67*, 11–17, doi:10.3311/PPch.21222.
6. Kravtsova, A.A.; Skuredina, A.A.; Malyshev, A.S.; Le-Deygen, I.M.; Kudryashova, E. V.; Budynina, E.M. The Solubility Studies and the Complexation Mechanism Investigations of Biologically Active Spiro[Cyclopropane-1,3′-Oxindoles] with β-Cyclodextrins. *Pharmaceutics* **2023**, *15*, 228, doi:10.3390/pharmaceutics15010228.
7. Zornoza, A.; Vélaz, I.; González-Gaitano, G.; Martínez-Ohárriz, M.C. A Comprehensive Study of Gemfibrozil Complexation with β-Cyclodextrins in Aqueous Solution Using Different Analytical Techniques. *Int. J. Mol. Sci.* **2022**, *23*, doi:10.3390/ijms232416119.
8. Soe, H.M.S.H.; Chamni, S.; Mahalapbutr, P.; Kongtaworn, N.; Rungrotmongkol, T.; Jansook, P. The Investigation of Binary and Ternary Sulfobutylether-β-Cyclodextrin Inclusion Complexes with Asiaticoside in Solution and in Solid State. *Carbohydr. Res.* **2020**, *498*, 108190, doi:10.1016/j.carres.2020.108190.
9. Censi, R.; Di Martino, P. Polymorph Impact on the Bioavailability and Stability of Poorly Soluble Drugs. *Molecules* **2015**, *20*, 18759–18776, doi:10.3390/molecules201018759.
10. Li, L.; Yin, X.-H.; Diao, K.-S. Improving the Solubility and Bioavailability of Pemafibrate via a New Polymorph Form II. *ACS Omega* **2020**, *5*, 26245–26252, doi:10.1021/acsomega.0c04005.
11. T. Loftsson, Z. Fulop, Patent US 11135311 B2.

12. Mentzafos, D.; Bethanis, K. ß-Cyclodextrin Dimeric Inclusion Complexes: A Review of Some Crystal Structure Aspects. In: *Cyclodextrins: Synthesis, Chemical Applications and Role in Drug Delivery*; Ramirez, F.G., Ed.; Nova Science: New York, USA, 2015; Chapter 8.
13. Ceborska, M. Structural Investigation of Solid State Host/Guest Complexes of Native Cyclodextrins with Monoterpenes and Their Simple Derivatives. *J. Mol. Struct.* **2018**, *1165*, 62–70, doi:10.1016/j.molstruc.2018.03.114.
14. Harata, K. Crystallographic Study of Cyclodextrins and Their Inclusion Complexes. In: *Cyclodextrins and Their Complexes: Chemistry, Analytical Methods, Applications*; Dodziuk, H.; Ed.; Wiley-VCH: Weinheim, Germany, 2006; pp. 147–198.
15. Shih, T.-W.; Hsu, C.-L.; Chen, L.-Y.; Huang, Y.-C.; Chen, C.-J.; Inoue, Y.; Sugiyama, T. Optical Trapping-Induced New Polymorphism of β-Cyclodextrin in Unsaturated Solution. *Cryst. Growth Des.* **2021**, *21*, 6913–6923, doi:10.1021/acs.cgd.1c00822.
16. Panova, I.G.; Zhukova, E.K.; Matukhina, E. V.; Topchieva, I.N. Receptor Properties of Nanoporous Structures Based on β-Cyclodextrin. *Nanotechnologies Russ.* **2010**, *5*, 304–312, doi:10.1134/S1995078010050046.
17. Panova, I.G.; Matukhina, E. V.; Gerasimov, V.I.; Topchieva, I.N. Non-Covalent Columnar Cyclodextrin-Based Structures. *Colloid J.* **2006**, *68*, 66–78, doi:10.1134/S1061933X06010091.
18. Ramos, A.I.; Braga, T.M.; Silva, P.; Fernandes, J.A.; Ribeiro-Claro, P.; Lopes, M. de F.S.; Paz, F.A.A.; Braga, S.S. Chloramphenicol·cyclodextrin Inclusion Compounds: Co-Dissolution and Mechanochemical Preparations and Antibacterial Action. *CrystEngComm* **2013**, *15*, 2822, doi:10.1039/c3ce26414a.
19. Steiner, T.; Koellner, G. Crystalline β-Cyclodextrin Hydrate at Various Humidities: Fast, Continuous, and Reversible Dehydration Studied by X-Ray Diffraction. *J. Am. Chem. Soc.* **1994**, *116*, 5122–5128, doi:10.1021/ja00091a014.
20. Sala, A.; Hoossen, Z.; Bacchi, A.; Caira, M.R. Two Crystal Forms of a Hydrated 2:1 β-Cyclodextrin Fluconazole Complex: Single Crystal X-Ray Structures, Dehydration Profiles, and Conditions for Their Individual Isolation. *Molecules* **2021**, *26*, 4427, doi:10.3390/molecules26154427.
21. Giordano, F.; Novak, C.; Moyano, J.R. Thermal Analysis of Cyclodextrins and Their Inclusion Compounds. *Thermochim. Acta* **2001**, *380*, 123–151, doi:10.1016/S0040-6031(01)00665-7.
22. Jansook, P.; Ogawa, N.; Loftsson, T. Cyclodextrins: Structure, Physicochemical Properties and Pharmaceutical Applications. *Int. J. Pharm.* **2018**, *535*, 272–284, doi:10.1016/j.ijpharm.2017.11.018.
23. Lan Pham, T.; Usacheva, T.R.; Alister, D.A.; Thu Ha Nguyen, T.; Tukumova, N.V.; Kuranova, N.N.; Minh Vu, X.; My Hanh Le, T.; Tung Nguyen, Q.; Lam Tran, D. Thermodynamic Parameters and Quantum Chemical Calculations of Complex Formation between Rutin and 2-Hydroxypropyl-β-Cyclodextrin in Water-Ethanol Solvents. *J. Mol. Liq.* **2022**, *366*, 120324, doi:10.1016/j.molliq.2022.120324.
24. Osel'skaya, V.Y.; Gatiatulin, A.K.; Klimovitskii, A.E.; Ziganshin, M.A.; Gorbatchuk, V. V. Competing Role of Water in Inclusion of Indomethacin and Volatile Organic Compounds by Native Cyclodextrins. *Macroheterocycles* **2022**, *15*, 174–185, doi:10.6060/mhc224319g.
25. Nagrimanov, R.N.; Samatov, A.A.; Buzyurov, A. V.; Kurshev, A.G.; Ziganshin, M.A.; Zaitsau, D.H.; Solomonov, B.N. Thermochemical Properties of Mono- and Di-Cyano-Aromatic Compounds at 298.15 K. *Thermochim. Acta* **2018**, *668*, 152–158, doi:10.1016/j.tca.2018.07.026.
26. Altomare, A.; Cuocci, C.; Giacovazzo, C.; Moliterni, A.; Rizzi, R.; Corriero, N.; Falcicchio, A. EXPO2013: A Kit of Tools for Phasing Crystal Structures from Powder Data. *J. Appl. Crystallogr.* **2013**, *46*, 1231–1235, doi:10.1107/S0021889813013113.
27. McCusker, L.B.; Von Dreele, R.B.; Cox, D.E.; Louër, D.; Scardi, P. Rietveld Refinement Guidelines. *J. Appl. Crystallogr.* **1999**, *32*, 36–50, doi:10.1107/S0021889898009856.
28. Varfolomeev, M.A.; Abaidullina, D.I.; Solomonov, B.N.; Verevkin, S.P.; Emel'yanenko, V.N. Pairwise Substitution Effects, Inter- and Intramolecular Hydrogen Bonds in Methoxyphenols and Dimethoxybenzenes. Thermochemistry, Calorimetry, and First-Principles Calculations. *J. Phys. Chem. B* **2010**, *114*, 16503–16516, doi:10.1021/jp108459r.
29. Vyazovkin, S. *Isoconversional Kinetics of Thermally Stimulated Processes*; Springer: Heidelberg, Germany, 2015; p. 239.
30. Vyazovkin, S.; Burnham, A.K.; Criado, J.M.; Pérez-Maqueda, L.A.; Popescu, C.; Sbirrazzuoli, N. ICTAC Kinetics Committee Recommendations for Performing Kinetic Computations on Thermal Analysis Data. *Thermochim. Acta* **2011**, *520*, 1–19, doi:10.1016/j.tca.2011.03.034.
31. Gatiatulin, A.K.; Grishin, I.A.; Buzyurov, A. V.; Mukhametzyanov, T.A.; Ziganshin, M.A.; Gorbatchuk, V. V. Determination of Melting Parameters of Cyclodextrins Using Fast Scanning Calorimetry. *Int. J. Mol. Sci.* **2022**, *23*, 13120, doi:10.3390/ijms232113120.

32. Gorbatchuk, V. V.; Gatiatulin, A.K.; Ziganshin, M.A.; Gubaidullin, A.T.; Yakimova, L.S. Unusually High Efficiency of β-Cyclodextrin Clathrate Preparation by Water-Free Solid-Phase Guest Exchange. *J. Phys. Chem. B* **2013**, *117*, 14544–14556, doi:10.1021/jp408059b.
33. Gatiatulin, A.K.; Ziganshin, M.A.; Yumaeva, G.F.; Gubaidullin, A.T.; Suwińska, K.; Gorbatchuk, V. V. Using Water-Mimic Organic Compounds to Activate Guest Inclusion by Initially Dry Beta-Cyclodextrin. *RSC Adv.* **2016**, *6*, 61984–61995, doi:10.1039/C6RA11378H.
34. Kayaert, P.; Li, B.; Jimidar, I.; Rombaut, P.; Ahssini, F.; Van den Mooter, G. Solution Calorimetry as an Alternative Approach for Dissolution Testing of Nanosuspensions. *Eur. J. Pharm. Biopharm.* **2010**, *76*, 507–513, doi:10.1016/j.ejpb.2010.09.009.
35. Bilal, M.; de Brauer, C.; Claudy, P.; Germain, P.; Letoffe, J. β-Cyclodextrin hydration: a calorimetric and gravimetric study. *Thermochim. Acta* **1995**, *249*, 63–73, doi:10.1016/0040-6031(94)01933-8.
36. Lindner, K.; Saenger, W. Crystal and Molecular Structure of Cyclohepta-Amylose Dodecahydrate. *Carbohydr. Res.* **1982**, *99*, 103–115, doi:10.1016/S0008-6215(00)81901-1.
37. Briggner, L.-E.; Wadsö, I. Heat Capacities of Maltose, Maltotriose, Maltotetrose and α-, β-, and γ-Cyclodextrin in the Solid State and in Dilute Aqueous Solution. *J. Chem. Thermodyn.* **1990**, *22*, 1067–1074, doi:10.1016/0021-9614(90)90156-K.
38. Burger, A.; Ramberger, R. On the Polymorphism of Pharmaceuticals and Other Molecular Crystals. I. *Mikrochim. Acta* **1979**, *72*, 259–271, doi:10.1007/BF01197379.
39. Gorbatchuk, V. V; Tsifarkin, A.G.; Antipin, I.S.; Solomonov, B.N.; Konovalov, A.I. Influence of the Guest Molecular Size on the Thermodynamic Parameters of Host–Guest Complexes between Solid Tert-Butylcalix[4]Arene and Vapours of Organic Compounds. *Mendeleev Commun.* **1999**, *9*, 11–13, doi:10.1070/MC1999v009n01ABEH000989.
40. Ogata, F.; Hayabuchi, R.; Saenjum, C.; Nakamura, T.; Kawasaki, N. Adsorption Behavior of Water on Virgin and Modified Cyclodextrin. *Yakugaku Zasshi* **2020**, *140*, 1165–1173, doi:10.1248/yakushi.20-00097.
41. Loftsson, T.; Sigurdsson, H.H.; Jansook, P. Anomalous Properties of Cyclodextrins and Their Complexes in Aqueous Solutions. *Materials (Basel).* **2023**, *16*, 2223, doi:10.3390/ma16062223.